DEVELOPMENT OF SPLIT-PROTEIN REASSEMBLY TOOLS TO STUDY KINASE FUNCTION

By

BENJAMIN JAMES ROUNSEVILLE

_____

A Thesis Submitted to The Honors College

In Partial Fulfillment of the Bachelors degree
With Honors in

Biochemistry

THE UNIVERSITY OF ARIZONA

M A Y 2 0 1 8

Approved by:

_____

Dr. Indraneel Ghosh
Department of Chemistry and Biochemistry

Table of Contents

Abstract:

To better study the role of a specific kinase and bypass the well-known challenge of selectively targeting kinases, we designed a ligand-gated split-protein system where two halves of a kinase are reassembled via the addition of a Chemical Inducer of Dimerization (CID) with concomitant activation of the enzyme. This was done by splitting the catalytic domain of tyrosine kinase Src into two inactive halves, and linking each to a copy of E. coli dihydrofolate reductase (eDHFR). Trimethoprim (TMP) is a tight and selective ligand for eDHFR, and in the presence of a di-TMP ligand, the previously mentioned Src-eDHFR halves dimerize, achieving reassembly into a functional kinase with measureable activity.

To demonstrate the use of our Src-eDHFR system *in cellulo*, we expressed the split-kinase in mammalian cells and measured overall phosphorylation via western blotting. We have shown that the activity of our Src-eDHFR system is dependent on the presence of the di-TMP ligand. In addition, we have shown that two well identified mutations (K298M and T341M) behave the same way in our split system as they do in the native, unaltered protein. Overall, our eDHFR-Src system seems able to replicate the function of Src *in cellulo*, giving future researchers a useful tool to elucidate the role Src plays in different cellular processes.

I. Introduction:

To pass on useful information from one generation of living organisms to the next, life has evolved a universal data storage system in the form of DNA. Within the base sequence of DNA, the instructions to synthesize all proteins are stored. Being able to manipulate this storage system gives scientists the ability to make very specific changes to the amino acid sequence and thus the overall structure of proteins. Using molecular cloning techniques, scientists have virtually no limits on what changes they can make. Once the changes have been made in the genetic information, the cell machinery does the work of translating the DNA into an actualized protein that can be studied. This process of protein engineering is a continuously expanding field with endless possibilities.

One area of interest in this field is the development and application of split-protein reassembly systems.[1,2] These systems utilize small molecular ligands called Chemical Inducers of Dimerization, or CIDs, to enable precise temporal control over the activity of a specific biological target. This biological target may be a kinase. Kinases are a class of enzyme that catalyze a phosphorylation reaction wherein a phosphate group is transferred from ATP to one of three amino acid residues: serine, threonine, or tyrosine.[3] The result of this reaction is often a structural change in the protein substrate that can cause a wide range of effects. Phosphorylation is a very important cellular process and plays a major role in signal transduction, cell division, and cell death.[4,5,6] Kinases are thus heavily researched and a common therapeutic target.

Kinases are very hard to selectively inhibit. This well-known problem arises from the fact that the 500+ kinases in the human kinome are homologous, meaning that they are evolutionarily closely related.[7] As a result, the structural characteristics of kinases are similar. This makes selectively inhibiting kinases a difficult procedure using traditional methods.[8] CID activated

split-kinases offer a unique way to exert control over a specific kinase that would otherwise be hard to achieve.[9]

In split-kinase systems, a kinase is dissected into two inactive halves. The split site is carefully chosen so the independent halves do not spontaneously reassemble. It is also critically important that two halves can reassemble into an active enzyme when brought into proximity. Once a suitable split site has been chosen, each half is independently linked to suitable protein pair that dimerizes with the addition of a specific CID. When the CID is added, the resulting dimerization brings the two kinase halves together. The kinase subsequently reassembles into a fully functional and active kinase.

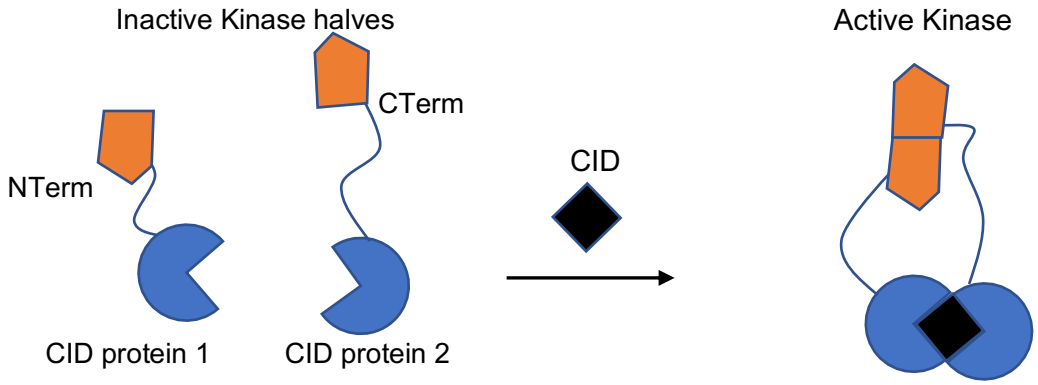

Figure 1: General schematic of CID activated split-kinase reassembly system. A kinase is split into an N-terminal half and a C-terminal half. Each half is independently linked to a CID interacting protein. When the CID is added, the CID interacting proteins dimerize which is followed by kinase reassembly and activation.

Identifying viable split sites requires a large amount of trial and error. The rationale behind the location of the split site relies heavily upon a sequence dissimilarity approach based on kinase sequence alignment. Using this approach, our lab has developed a variety of split-kinase systems. These systems utilize CIDs such as rapamycin, abscisic acid, and gibberellic acid.[10,11] These naturally occurring CIDs are widely used in the signaling community.[12,13,14] While it has been shown that these CID systems are capable of reassembling and activating a

wide number kinases with temporal precision, dissembling the kinase once it has been CID activated remains elusive. **Figure 2** shows the results of previous experiments done by other lab members that demonstrate the lack of reversibility. Kinase activity was measured without the CID, after CID addition, and after a series of 6 washes. The results demonstrate that there is a well-defined activation with the addition of the CID. However, no significant deactivation is observed after the washes.

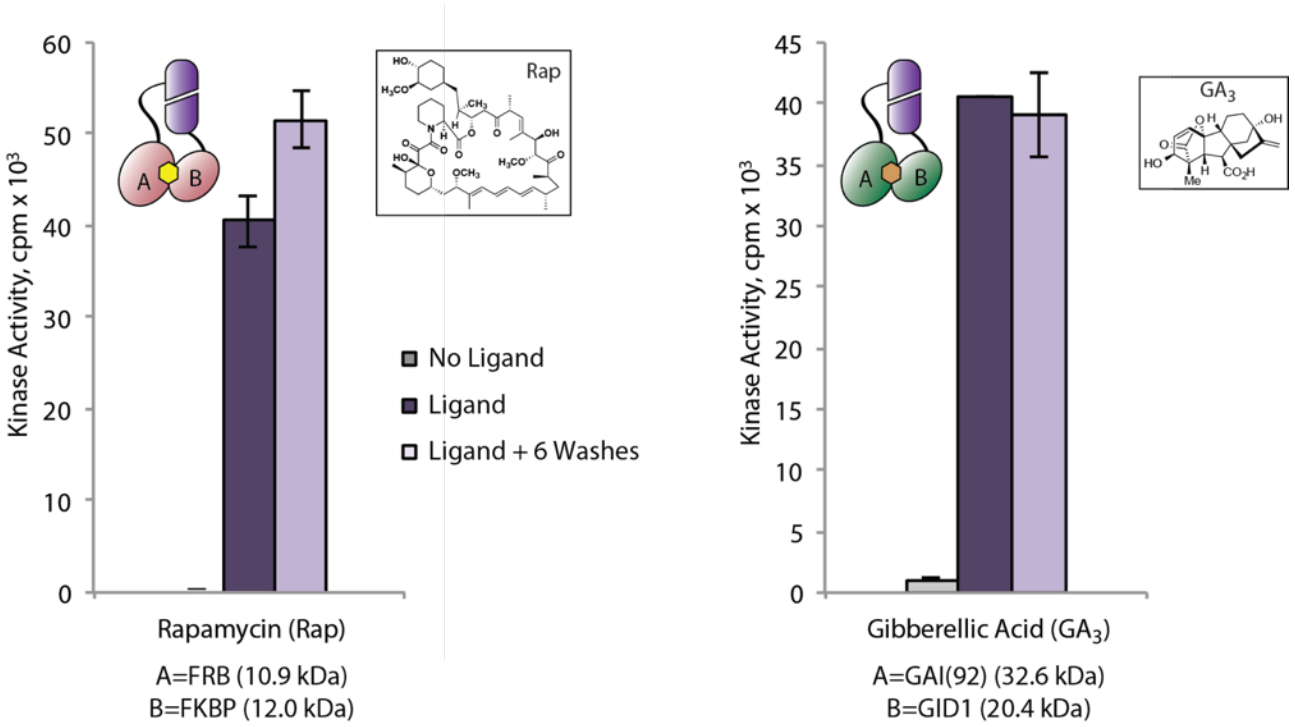

Figure 2: Activity assay of two different split-Lyn systems. Kinase activity was measured without CID, with CID, and with CID after 6 washes. Activity is induced, but is irreversible. Figure used with permission from Dr. Javier Montoya-Castillo.[15]

To solve this apparent problem of reversibility, our lab decided to create a split-system utilizing a synthetic CID. The CID design is based on a di-trimethoprim scaffold and contains a photocleavable group that can be severed with a specific wavelength of light. In theory, cleavage of the CID would be followed by separation and disassembly of the kinase. Dihydrofolate reductase (DHFR) is a small protein containing 159 amino acids that binds tightly and selectively

to trimethoprim (TMP)[16]. Copies of DHFR were independently linked to the two inactive kinase halves. The photocleavable diTMP molecule (Caged-diTMP) can bind exactly two copies of DHFR, allowing it to act as a viable CID. DHFR from *E. coli* (eDHFR) binds to TMP 3,000 times tighter than mammalian DHFR.[17] Since our system will eventually be used to study mammalian cell biology, eDHFR has the advantage of being orthogonal to mammalian DHFR, making it an optimal choice.

The kinase used in our split system is the tyrosine kinase Src. Overexpression of Src has been correlated to growth and potency of various human cancers.[18,19] Src shares strong structural homology with 9 other tyrosine kinases. Together, these make up a group referred to as Src family kinases. Viable split sites for various kinases in this family have been reported by Hahn and co-workers.[20] Using this work as a template, a viable split site of Src was chosen. Once this site was chosen, a 25-amino acid linker was introduced to connect each kinase half to a copy of eDHFR.

In making a split-kinase system, one necessarily creates many changes to the parent kinase. The kinase is split into two, and the halves are linked to separate proteins. These changes have the potential to significantly alter the behavior of the kinase. Even if kinase activity is restored when the two halves reassemble, it must be shown that the split system behaves the same way as the unaltered parent kinase before it can be used to accurately study biology. To determine the fidelity of our split-Src system to unaltered variants of Src, a variety of well-known mutations were introduced. The behavior of these mutations in the split-system was compared to the behavior of the same mutations in unaltered variants of Src. If the mutations show the same behavior across each variant of Src, it is likely the split-Src system is an accurate model that can replicate the behavior of the parent Src. The first mutation is a deactivating that

changes a catalytic lysine to a methionine (K298M).[21] The other mutation we tested is an activating mutation (T341M).[22] Kinase activity was qualitatively measured using a cellular assay that measured overall global phosphorylation inside a cell.

For simplicity's sake, we began this project by splitting the catalytic domain of Src. The full-length version of this system is more complicated to work with as it contains several regulatory domains. To see any activity from the full length Src, a mutation (Y530F) needed to be incorporated.[23] Any cellular assay using the full-length version of Src, split or non-split, must contain this mutation. Once we can show that the split-catalytic Src behaves as expected inside a cell, the full-length version will be optimized. Work on the split full-length version has been started, and is at a preliminary stage.

In addition to measuring the activity of our system compared to unaltered variants of Src, we were interested in seeing the location of our system within a cell. We also wanted to use microscopy to measure the colocalization that occurs when the two halves are induced to dimerize. To do this, we linked small protein fluorophores to the N-terminal and C-terminal constructs and transfected them into HEK293T cells. We chose two very common fluorophores: eGFP and mCherry.[23,24] Cells containing these fluorophores can be excited and imaged via microscopy. Using a 3i Spinning Disk confocal microscope, we excited transfected cells with two wavelengths of laser and captured high-quality fluorescent images.

These preliminary colocalization experiments were done using a rapamycin based split-Src system. In this system, Src is split and linked to an FRB and FKBP protein pair. Upon addition of rapamycin, FRB and FKBP dimerize. Fluorophore eGFP was added to the N-terminal side and mCherry to the C-terminal side. To visualize the effect of adding rapamycin, a time lapse was performed where images were captured in 10 minute increments after rapamycin was

added. Since eGFP and mCherry are visualized at different wavelengths, we could determine relative expression levels and general cellular location of each half.

II. Materials and Methods:

Obtaining Plasmids:

pcDNA3.1(+) expression vectors containing the genes for each of the constructs being studied were obtained using standard cloning techniques. Many of the plasmids were available from previous work by other lab members. Some plasmids had to be generated by the author. The precursors to many of the cloned plasmids were the vectors *pcDNA3.1-MCS-25aa-DHFR* and *pcDNA3.1-DHFR- 27aa-MCS*. The MCS is a multiple cloning site that contains various restriction sites. In these vectors, the MCS was opened by digesting it at NheI/HindIII and EcoRV/KpNI restriction sites, respectively. Inserts containing a portion of the Src gene were then added. The inserts were obtained from the vector *pcDNA3.1- Kz-CFluc-Src(FL)(Y530F)* using PCR amplification. This was done by using primers designed to sit just outside the portion of the gene that was desired. One insert contained the portion of the gene coding for the N-terminal half and the other insert contained the gene coding for the C-terminal half.

The inserts were ligated into their respective vector using T4 DNA ligase and transformed into X1 blue *E. coli* cells through electroporation. A PCR screen was performed on the resulting colonies. The PCR screen uses general primers to generate a product equal to the entire gene contained within the pcDNA3.1 expression vector. The relative size of this product gives a good idea about whether the insert was added successfully. A negative control of the original vector without the insert was screened to determine positive and negative hits. Positive hits containing the insert are longer in length and thus do not migrate as far on the gel as negative hits as shown in **Figure 3**. Positive hits were collected and sent for high-throughput sequencing

for further confirmation. The same process was used to obtained vectors containing fluorescent protein tags used in the microscopy experiments.

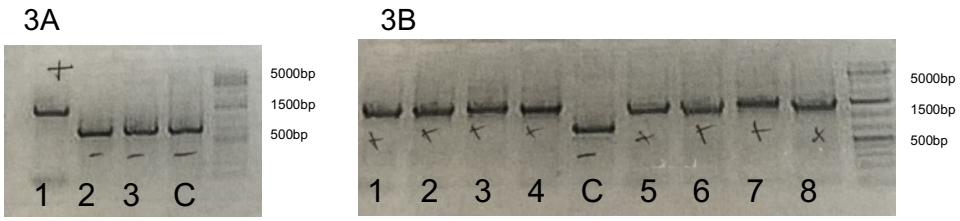

Figure 3A: PCR screen of bacteria colonies pcDNA3.1 *kz-NSrc(FL)268-25aa-eDHFR-H6*. Positive hits that contain the insert (in green) contain 1434 bp. Negative hits without the insert are 831 bp. Column 1 is a positive hit. **3B** is a PCR screen of *pcDNA3.1 kz-eDHFR-27aa-CSrc(Cat)268-H6(Y530F)*. Positive hits are 1320 bp and negative hits are 838 bp. All 8 samples are positive hits.

Site-directed mutagenesis was used to introduce the deactivating and activating mutations. Primers containing the instructions for the mutation were designed to overlap the area of the gene containing the amino acid we wanted to mutate. PCR using Kapa HiFi DNA polymerase was used to generate the mutant plasmids. All mutants were sequenced using high-throughput sequencing to confirm the presence of the mutation.

The following table is a list of the plasmids used in the following experiments. Mutagenesis was performed on the first six plasmids listen below to obtain a version with the deactivating (K298M) mutation and a version with the activating (T341M) mutations.

Table 1:

Vector name:	**Description:**
pcDNA3.1 kz-Src(Cat)-H6	Src catalytic domain with a poly-His tag
pcDNA3.1 kz-SrcFL-H6 (Y530F)	Src full length, containing catalytic and regulatory domains and a poly-His tag
pcDNA3.1 kz-NSrc(Cat)291-25aa-eDHFR	N-terminal portion of Src(Cat) linked to a copy of eDHFR
pcDNA3.1 kz-eDHFR-27aa-CSrc292-H6	C-terminal portion of Src(Cat) linked to a copy of eDHFR. Contains His-tag
pcDNA3.1 kz-NSrc(FL)268-25aa-eDHFR	N-terminal portion of SrcFL linked to a copy of eDHFR
pcDNA3.1 kz-eDHFR-27aa-CSrc268-H6 (Y530F)	C-terminal portion of Src linked to a copy of eDHFR. Contains His-tag

Table 1 continued:

Vector name:	Description:
pcDNA3.1 kz-eGFP-Src(Cat)-H6	Src catalytic domain connected to a eGFP fluorescence tag
pcDNA3.1 kz-eGFP-NSrc(Cat)268-13aa-FRB	N-terminal portion of Src(Cat) connected to a copy of FRB and a eGFP fluorescence tag
pcDNA3.1 kz-mCherry-FKBP-13aa-CSrc268-H6	C-terminal portion of Src connected to a copy of FKBP and an mCherry fluorescence tag.

Western Blots:

To measure the activity of our various Src constructs, we performed a cellular assay to measure overall global phosphorylation within a cell. Plasmids were transfected into live HEK293T cells using Polyjet In Vitro DNA transfection reagent. We transfected anywhere between 50 ng to 2 µg of plasmid and typically used 1-2 million HEK293T cells per sample. After 24 hours, 400 nM of Caged-diTMP was added. After 24 hours with the CID, the cells were lysed using mammalian protein extraction reagent containing protease and phosphatase inhibitors. The cellular debris was separated from the cell lysate via centrifugation. The protein content of the resulting supernatant was determined using BCA reagent and 20 µg of protein was run on a sodium dodecyl sulfate-polyacrylamide gel electrophoresis (SDS-PAGE) that separated proteins by size. The proteins of the gel were transferred to a poly-vinylidene difluoride (PVDF) membrane.

The PVDF membrane was incubated with appropriate primary and secondary antibodies. Primary antibodies included 1:1,000 dilution of mouse monoclonal anti-phosphotyrosine, 1:500

dilution of rabbit polyclonal anti-β-tubulin, and 1: 1,000 dilution of rabbit monoclonal anti-His tag. Photo-excitable secondary antibodies attach to the corresponding primary antibodies. After being incubated with primary antibodies, we treated the PVDF membrane to a 1: 2,000 dilution of goat anti-mouse IgG Alexa Fluor 647 and goat anti-rabbit igG Alexa Fluor 555 secondary antibodies. After being incubated with the secondary antibodies, the membrane was imaged using a Typhoon 9400 fluorescence scanner.

Imaging Cells:

Cells were plated on a cell imaging dish using High Glucose FluoroBrite DMEM supplemented with pyruvate and L-glutamine. 200 ng of each *kz-eGFP-NSrc(Cat)268-13aa-FRB* and *pcDNA3.1 kz-mCherry-FKBP-13aa-CSrc268-H6* was transfected using Polyjet In Vitro DNA transfection reagent. The microscope had a temperature-controlled platform that maintained cells at 37ºC. Once cells were focused using a 63x/1.4 objective, 1 µL of 100 µM of rapamycin was added, resulting in a 100 nM final rapamycin concentration in the media. Cells were excited using a 488 nm and a 561 nm laser. The 488 nm wavelength excited eGFP and the 561 nm wavelength excited mCherry. Images were collected every 10 minutes for a total of 4 hours.

III. Results/Discussion

The effect of the K298M and T341M mutations on different variants of Src is shown in **Figures 4 and 5**. The three images in each figure are of three targets identified by the different primary antibodies. The phosphotyrosine antibodies attached to phosphorylated tyrosine residues and provided a measure of overall phosphorylation within the cell. β-tubulin is a ubiquitous structural protein found in virtually all cells and was used as a loading control to verify protein is normalized across samples. Polyhistidine antibodies target the exogenous proteins containing His tags and provide direct confirmation that the transfected plasmids were translated and present in the cell lysate.

Figure 4 demonstrates that the behavior of the deactivating mutation is consistent across Src(Cat), Src(FL), and eDHFR-268-Src(Cat). There is a clear halting of *in cellulo* phosphorylation when the K298M mutation is introduced. The poly-His image proves that the knockout of phosphorylation can be attributed to the K298M mutation because the level of exogenous protein remains relatively constant between the (+/-) K298M lanes. For the split-system, the His tag is present on the C-terminal half only. Despite not having a direct evidence for the presence of the N-terminal side, we can be relatively certain that changes in phosphorylation are attributed to the split-system. Interestingly, the (+) CID lane seems to show slightly more signal in the poly-His image, suggesting that the CID may protect the halves from degradation. **Figure 5** shows that the T341M mutation behaves as expected in all 3 variants of Src. For the split-system, the increase in activity is from the T341M mutation is dependent on the presence of the CID.

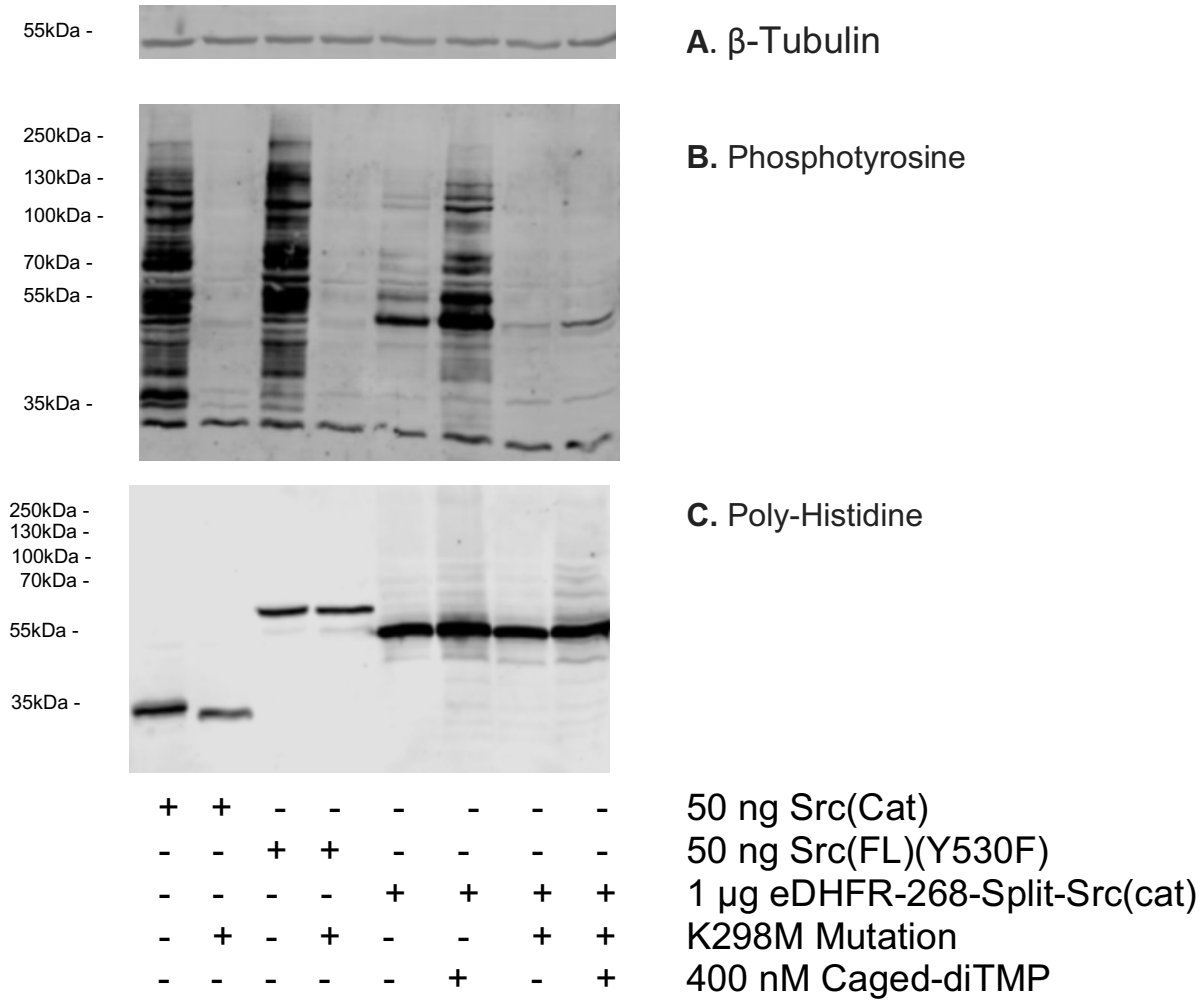

Figure 4. The effect of deactivating K298M mutation on *in cellulo* phosphorylation. **Fig. 4A** shows β-tubulin content in each lane confirming that each lane contains a normalized amount of protein. **Fig. 4B** shows the amount of phosphorylation from different variants of Src. Lanes 1-4 demonstrates the clear deactivating effect of K298M on the catalytic domain and full-length variant of Src. Lanes 5-6 show that activity is dependent on the presence of Caged-diTMP. Lanes 7-8 show that K298M kills activity in the split system regardless of the presence of the CID. **Fig. 4C** shows exogenous proteins containing a poly histidine tag. The weight of *Src(cat)-H6* is 35.4 kDA, *Src(FL)-H6* is 60.6kDa, and *eDHFR-25aa-CSrc(cat)268-H6* is 49.2kDa. The changes in phosphotyrosine signal are attributed to the His-tagged exogenous proteins.

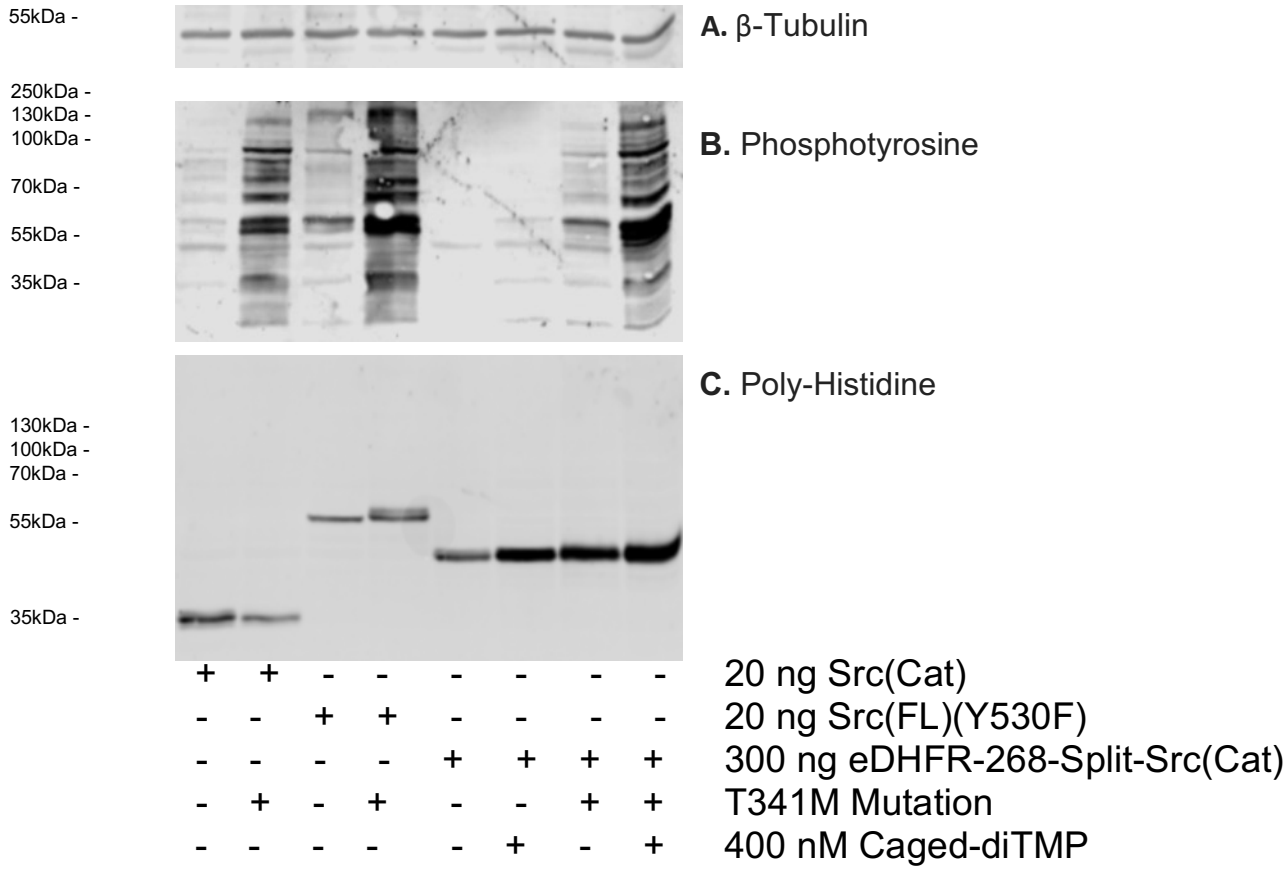

Figure 5. The effect of activating T341M mutation on *in cellulo* phosphorylation. **Fig. 5A** shows β-tubulin content in each lane confirming that each lane contains a normalized amount of protein. **Fig. 5B** shows the amount of phosphorylation from different variants of Src. Lanes 1-4 demonstrates the clear activating effect of T341M on the catalytic domain and full-length variant of Src. Lanes 5-8 show that T341 increases activity in the split-system but that this activity is dependent on the presence of the CID. **Fig. 5C** shows exogenous proteins containing a poly-histidine tag. The weight of *Src(Cat)-H6* is 35.4 kDa, *Src(FL)-H6* is 60.6kDa, and *eDHFR-25aa-CSrc(Cat)268-H6* is 49.2kDa. The changes in phosphotyrosine signal are attributed to the His-tagged exogenous proteins.

In addition to working with the split-catalytic system, we wanted to begin optimizing the split-full length version. We began by seeing if we could induce an increase in activity in the split-full length system with the addition of a CID comparable to the split-catalytic system. **Figure 6** shows preliminary results of a three-step titration of Caged-diTMP on the split-catalytic and split-full length systems. The catalytic system shows incremental increase in activity as the CID concentration is increased. The full-length version has a subtler increase in activity. Unfortunately, these preliminary results show that the full-length version of split-Src will need to be further optimized before it can be used to model unaltered Src.

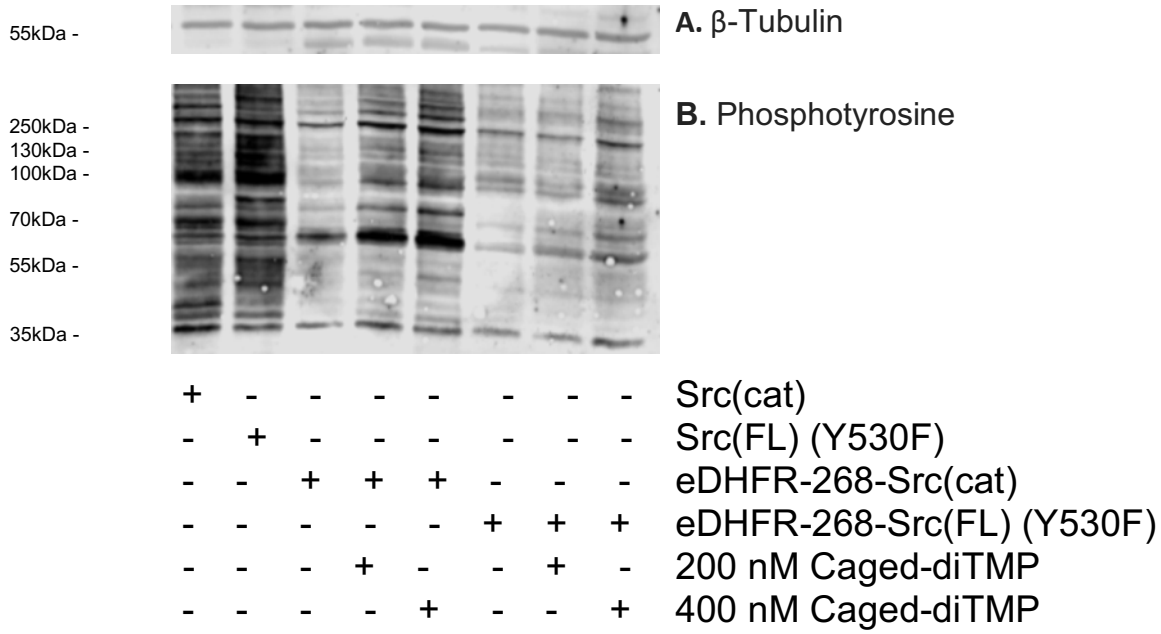

Figure 6. Comparison of a titration between split-Src(Cat) and split-Src(FL). Increasing CID concentration has an observable increase on activity for the split-catalytic system. The increase in activity for the split-full length system is less pronounced.

Cell Imaging:

Before any fluorescent imaging experiments were begun, an assay to verify the viability of the split-system containing fused fluorophores was performed (**Figure 7)**. This was done on a split-Src system based on the CID rapamycin. A non-split version of Src(Cat) with and without a GFP tag was also tested. The split rapamycin system consisted of *pcDNA3.1 kz-[eGFP]-NSrc(Cat)268-13aa-FRB* and *pcDNA3.1 kz-[mCherry]-13aa-CSrc(Cat)268-H6.* The cellular assay was performed on constructs with and without the fused fluorophores. The results show a clear increase in activity upon addition of rapamycin regardless of the presence of fused fluorophores indicating that the fluorophores do not seem to interfere with the kinase activity.

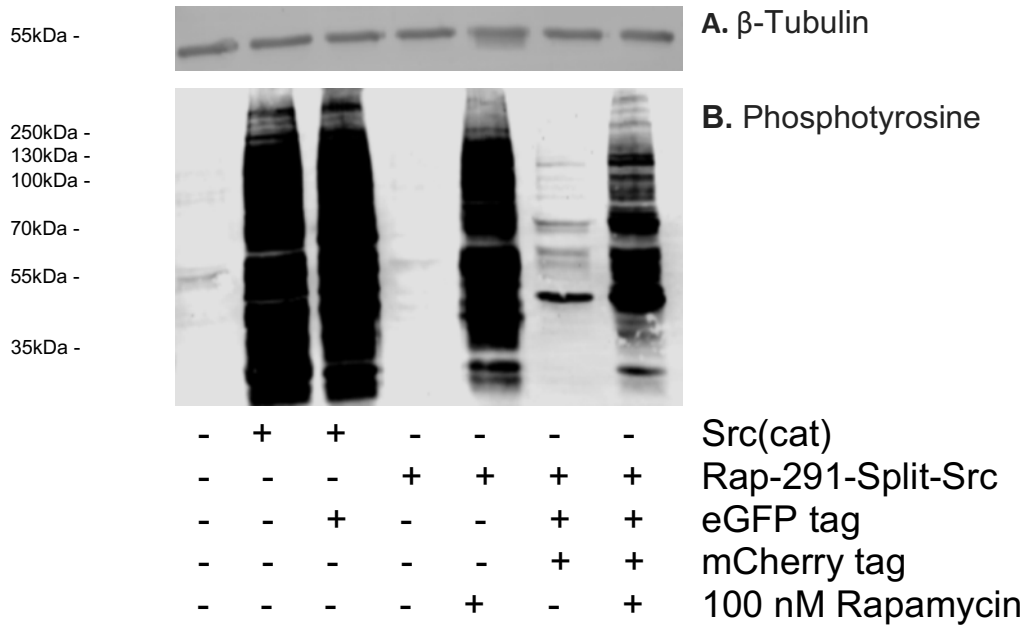

Figure 7. Cellular assay of rapamycin split-Src system with and without fused fluorophores. The presence of eGFP and mCherry on the non-split catalytic Src and split Src has no obvious interference on activity. For the split system, kinase activity is dependent on CID with and without the fluorophores.

Once we confirmed that the fluorophores do not obstruct the split system, cells were transfected with both halves of rapamycin-split Src and were imaged using a 3i Spinning Disk confocal microscope. Fluorescent images from two laser wavelengths were collected every 10 minutes after the addition of rapamycin. **Figure 8** shows four cells containing fluorescent activity. The cells are labeled 1-4. Cell 2 is predominantly green, meaning it mostly received the plasmid encoding the N-terminal half tagged with GFP. Likewise, cell 3 is predominately red, meaning it mostly received the plasmid encoding the C-terminal half tagged with mCherry. Cells 1 and 4 have a more orange and yellow appearance meaning they were co-transfected and received both plasmid halves. This suggests that the transfection process may be slightly inefficient or inconsistent.

Interestingly, the intensity of fluorescence increases after the addition of rapamycin. This is especially pronounced with the mCherry signal in cells 1 and 3. More controls such as transfecting and imaging each half separately with and without rapamycin will need to be carried out, but one hypothesis explaining this phenomenon is rapamycin prevents the halves from being degraded. The idea that the CID stabilizes either half of the split and prevents degradation is supported by the poly-histidine images in **Figures 4 and 5**. The signal is stronger in the lanes containing the CID. This may force us to reconsider the way in which we believe the CID activates our split-kinases. Rather than inducing dimerization of the linked CID interacting proteins which in turn induces kinase reformation and reactivation, the CID may simply prevent the split-kinase from degrading after being translated. The most probable explanation is that the CID reactivates the enzyme by a combination of both phenomena. The CID both reassembles the protein halves into a functional enzyme *and* protects newly translated protein from degradation.

Both factors contribute to an increased concentration of reactivated kinase and thus an increase in cellular phosphorylation.

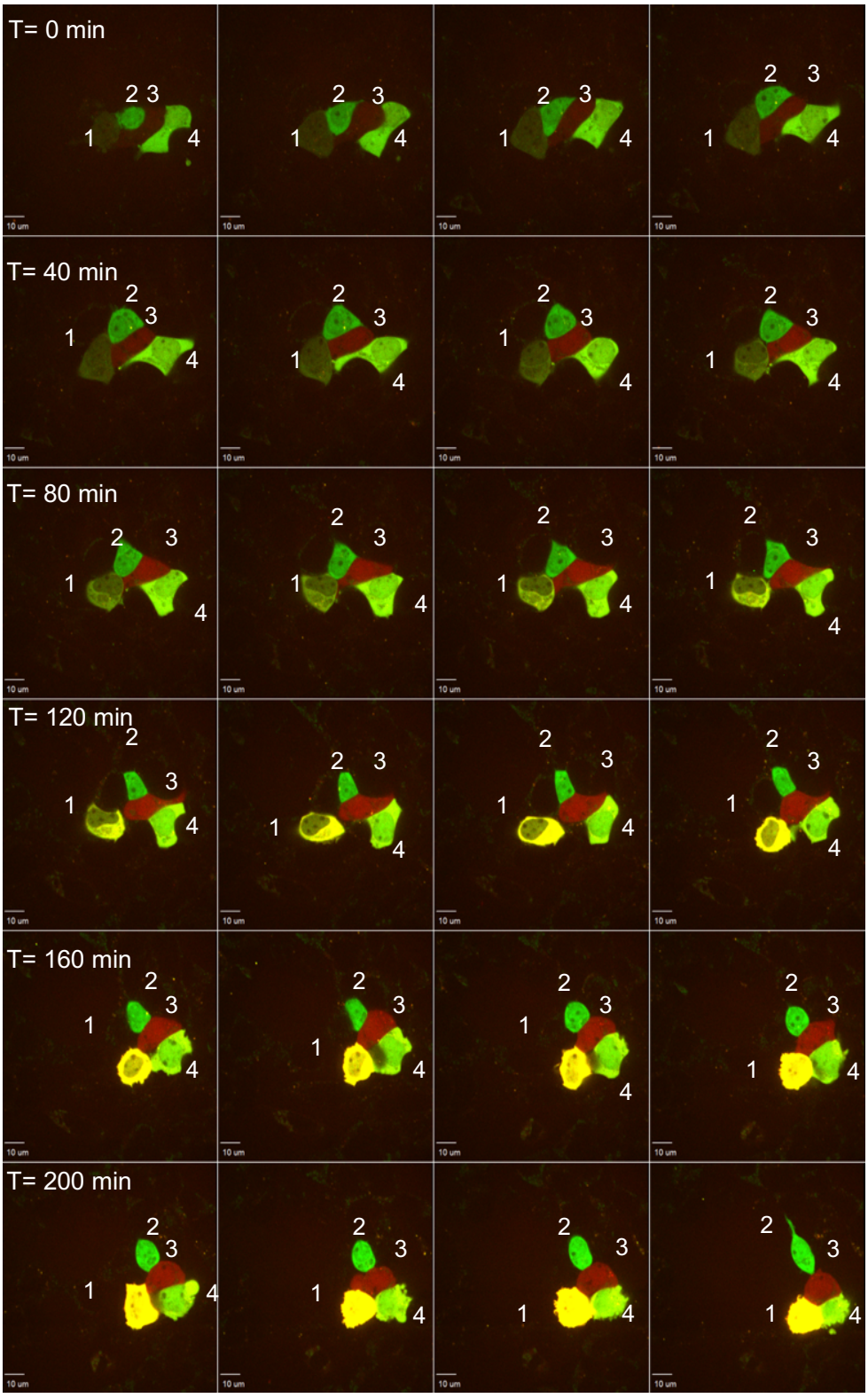

Figure 8. Cells excited with 488 nm and 561 nm lasers. After 1 µL of 100 µM rapamycin was added, images were captured every 10 minutes. Cells containing fluorescent activity are labeled 1-4.

IV. Conclusion:

It has been shown that our eDHFR-Src(Cat) split-kinase system can be expressed in cells and induced to increase *in cellulo* phosphorylation in a consistent and measurable manner via the addition of a small molecule CID. Furthermore, the character of two well-known mutations has been shown to behave predictably in our split-system. The consistent behavior of these mutations across Src(Cat), Src(FL) and eDHFR-Src(Cat) demonstrate the procedure of splitting Src does not alter its characteristic behavior in any fundamental way. Work can now proceed to optimize kinase deactivation via the photocleavable functional group in our CID. In addition, a split-Src(FL) system can now be optimized. **Figure 6** shows that the split-full length system is subtly activated with addition of the CID. This can be optimized by changing various conditions such concentration of CID, amount of plasmid transfected, and antibody concentration. Getting a full-length version of our system working will offer future researchers a useful tool to study the role Src plays in various signaling pathways.

The microscopy of our split-system provides additional insights about the split-system that can aide in the development and optimization of future split-kinase systems. So far, it has given us an idea about the overall expression level of our system within a cell and how that level changes over time. Continuing to monitor and study how the expression level changes over time and under various conditions will give us a better idea about the timeframe in which our system becomes active. This information will help us optimize split-kinase systems that will be used to by future researchers to elucidate the role kinases play in different cellular processes.

V. Acknowledgements:

First and foremost, I would like to thank Dr. Javier Castillo-Montoya for his constant training and mentorship. I would also like to thank Dr. Ghosh and all the members of the lab group for their support and helpful discussions.

VI. References:

1. Shekhawat, Sujan S., and Indraneel Ghosh. "Split-protein systems: beyond binary protein–protein interactions." Current opinion in chemical biology 15.6 (2011): 789-797.
2. Gray, Nathanael S., et al. "Exploiting chemical libraries, structure, and genomics in the search for kinase inhibitors." Science 281.5376 (1998): 533-538.
3. Manning, Gerard, et al. "The protein kinase complement of the human genome." Science 298.5600 (2002): 1912-1934.
4. Parsons, Sarah J., and J. Thomas Parsons. "Src family kinases, key regulators of signal transduction." *Oncogene* 23.48 (2004): 7906-7909.
5. Roche, Serge, Stefano Fumagalli, and Sara A. Courtneidge. "Requirement for Src family protein tyrosine kinases in G2 for fibroblast cell division." *Science* 269.5230 (1995): 1567.
6. Aikawa, Ryuichi, et al. "Oxidative stress activates extracellular signal-regulated kinases through Src and Ras in cultured cardiac myocytes of neonatal rats." *Journal of Clinical Investigation* 100.7 (1997): 1813.
7. Irby, Rosalyn B., and Timothy J. Yeatman. "Role of Src expression and activation in human cancer." Oncogene 19.49 (2000).
8. Hanke, Jeffrey H., et al. "Discovery of a novel, potent, and Src family-selective tyrosine kinase inhibitor Study of Lck-and FynT-dependent T cell activation." *Journal of Biological Chemistry* 271.2 (1996): 695-701.
9. Druker, Brian J., and Nicholas B. Lydon. "Lessons learned from the development of an abl tyrosine kinase inhibitor for chronic myelogenous leukemia." The Journal of clinical investigation 105.1 (2000): 3-7.
10. Camacho-Soto, Karla, et al. "Small molecule gated split-tyrosine phosphatases and orthogonal split-tyrosine kinases." Journal of the American Chemical Society 136.49 (2014): 17078-17086.
11. Camacho-Soto, Karla, et al. "Ligand-gated split-kinases." Journal of the American Chemical Society 136.10 (2014): 3995-4002.
12. Vezina, Claude, Alicia Kudelski, and S. N. Sehgal. "Rapamycin (AY-22, 989), a new antifungal antibiotic." The Journal of antibiotics 28.10 (1975): 721-726.

13. Santner, Aaron, and Mark Estelle. "Recent advances and emerging trends in plant hormone signalling." Nature 459.7250 (2009): 1071-1078.
14. Santiago, Julia, et al. "The abscisic acid receptor PYR1 in complex with abscisic acid." Nature 462.7273 (2009): 665-668.
15. Castillo-Montoya, J. (2016) *Development of Orthogonal Split-Kinase and Split-Phosphatase Systems for Interrogating and Rewiring Signal Transduction*. Doctoral thesis.)
16. Baker, D. J., et al. "The binding of trimethoprim to bacterial dihydrofolate reductase." *FEBS letters* 126.1 (1981): 49-52.
17. Dauber-Osguthorpe, Pnina, et al. "Structure and energetics of ligand binding to proteins: Escherichia coli dihydrofolate reductase-trimethoprim, a drug-receptor system." Proteins: Structure, Function, and Bioinformatics 4.1 (1988): 31-47.
18. Irby, Rosalyn B., and Timothy J. Yeatman. "Role of Src expression and activation in human cancer." Oncogene 19.49 (2000): 5636.
19. Wheeler, Deric L., Mari Iida, and Emily F. Dunn. "The role of Src in solid tumors." The oncologist 14.7 (2009): 667-678.
20. Karginov, A. V., Ding, F., Kota, P., Dokholyan, N. V., & Hahn, K. M. (2010). Engineered allosteric activation of kinases in living cells. Nature Biotechnology, 28(7), 743–747.
21. Russo, M. W., et al. "Identification of residues in the nucleotide binding site of the epidermal growth factor receptor/kinase." *Journal of Biological Chemistry* 260.9 (1985): 5205-5208.
22. Azam, Mohammad, et al. "Activation of tyrosine kinases by mutation of the gatekeeper threonine." Nature structural & molecular biology 15.10 (2008): 1109-1118.
23. Wei, Xunbin, et al. "Real-time imaging of nuclear permeation by EGFP in single intact cells." *Biophysical journal* 84.2 (2003): 1317-1327.
24. Tramier, Marc, et al. "Sensitivity of CFP/YFP and GFP/mCherry pairs to donor photobleaching on FRET determination by fluorescence lifetime imaging microscopy in living cells." *Microscopy research and technique* 69.11 (2006): 933-939.